Published in final edited form as:
Nanotoxicology. 2011 December ; 5(4): 459–468. doi:10.3109/17435390.2010.516026.

Biodistribution and acute toxicity of naked gold nanoparticles in a rabbit hepatic tumor model

EVAN S GLAZER[1], **CIHUI ZHU**[1], **AMIR N. HAMIR**[2], **AGATHA BORNE**[2], **C. SHEA THOMPSON**[1,3], and **STEVEN A. CURLEY**[1,4,*]

EVAN S GLAZER: eglazer@mdanderson.org; CIHUI ZHU: cizhu@mdanderson.org; AMIR N. HAMIR: ahamir@mdanderson.org; AGATHA BORNE: atborne@mdanderson.org; C. SHEA THOMPSON: ct4@rice.edu

[1]Department of Surgical Oncology, The University of Texas M. D. Anderson Cancer Center, Houston, TX

[2]Department of Veterinary Medicine and Surgery, The University of Texas M. D. Anderson Cancer Center, Houston, TX

[3]Department of Biomedical Engineering, Rice University, Houston, TX

[4]Department of Mechanical Engineering and Materials Science, Rice University, Houston, TX

Abstract

There is a paucity of data regarding the safety of administering solid gold nanoparticles (AuNPs) in large animal tumor models. We assessed the acute toxicity and biodistribution of 5 nm and 25 nm solid AuNPs in New Zealand White rabbits (n = 6 in each) with implanted liver Vx2 tumors 24 hours after intravenous injection. Gold concentration was determined by inductively coupled plasma atomic emission spectrometry (ICP) and imaged with transmission electron microscopy (TEM). There was no clinico-pathologic evidence of renal, hepatic, pulmonary, or other organ dysfunction. After 25 nm AuNP administration, the concentration of white blood cells increased after treatment ($p = 0.001$). Most other blood studies were unchanged. AuNPs were distributed to the spleen, liver, and Vx2 tumors, but not to other tissues. The urinary excretion of AuNPs was bimodal as measured by ICP. 25 nm AuNPs were more evenly distributed throughout tissues and may be better tools for medical therapy.

Keywords

gold nanoparticle; tumor model; biodistribution; acute toxicity

Introduction

Nanoparticles of many shapes, sizes, and components are rapidly moving from the basic science laboratory into the arena of clinical biomedical research. These nanoparticles are typically on the order of tens of nanometers to hundreds of micrometers in size (Ibrahim,

*Corresponding author Steven A. Curley, M.D., 1400 Holcombe Blvd, Unit 444, Houston, TX 77030, scurley@mdanderson.org, Phone: 713-794-4957, Fax: 713-745-5235.

We have no conflicts of interest.

Author contributions

ESG & SAC designed the experiments and wrote the manuscript.
ESG, CZ, ANH, AB, and CST performed the experiments.
ESG and ANH analyzed the data.
All authors were involved in editing the final manuscript and approved its final form.

Desai et al. 2002; Wust, Gneveckow et al. 2006; Curley, Cherukuri et al. 2008; Chien, Illi et al. 2009). Of the many forms of nanoparticles, some of the most clinically useful appear to be solid gold nanoparticles (AuNP) because of the presumed but yet unproven safety, the relatively simple and well described chemical reactions with gold, and relative ease of making defined sizes of these nanoparticles (Cherukuri, Glazer et al. 2009). In addition, the ability to conjugate multiple components in a AuNP-based construct permit varied uses with targeting antibodies, fluorophores, magnetic particles, toxins, etc. (Cherukuri, Glazer et al. 2009; Dhar, Daniel et al. 2009; Glazer and Curley 2010). Multiple forms of gold salts have been used clinically to treat rheumatoid arthritis (Finkelstein, Walz et al. 1976) and recent early studies using gold in cancer treatment have been reported (Milacic, Fregona et al. 2008). The major toxicity associated with gold salt therapy is renal via direct interaction between renal tubules and gold ions (Antonovych 1981). However, metallic AuNP may behave differently compared to gold salts due to differences in their size, shape, and chemical properties.

Tumor neovasculature is very important in the distribution of nanoparticles. Although varying by tumor size, location, cell type, primary versus metastatic lesion, and host factors, tumor vessels are on average 40 μm in diameter with a range up to 220 μm (Hashizume, Baluk et al. 2000). Nearly 50% of tumor blood vessels were less than 25 μm in diameter in this analysis (Hashizume, Baluk et al. 2000). Furthermore, the median pore or fenestration size in the endothelial wall was 1.5 μm.

Previously, other groups have described the internalization of AuNPs *in vitro,* (Chithrani, Ghazani et al. 2006) while others described theoretical models of receptor mediated endocytosis (Decuzzi and Ferrari 2008). Both suggest that peak internalization occurs when the construct is on the order of approximately 50 nm in diameter. This fits very well with the measured pore size in some cancer models. As an example, if the typical targeting antibody has a hydrodynamic diameter of approximately 10–20 nm (Sukumar, Doyle et al. 2004), then the “ideal” gold nanoparticle is approximately 5 nm to 25 nm in diameter, depending on the size, shape, and number of targeting proteins that bind to each AuNP. Although there have been some experiments *in vivo,* (De Jong, Hagens et al. 2008; Sonavane, Tomoda et al. 2008; Bar-Ilan, Albrecht et al. 2009) larger animals have not been adequately evaluated for both biodistribution and acute toxicity following delivery of AuNPs.

We hypothesize that naked (not conjugated to proteins, polymers, or linkers) gold nanoparticles will be distributed and excreted in a size-specific manner. Therefore, we investigated the biodistribution, pharmacokinetics, and acute toxicity of citrate-stabilized solid gold nanoparticles in New Zealand White rabbits.

Materials & Methods

Gold nanoparticles, Vx2 tumor, and animals

Two sizes of citrate-stabilized AuNP (Ted Pella, Inc., Redding, CA) were confirmed with transmission electron microscopy (TEM, Figure 1) and dynamic light scattering (DLS, n = 3 samples, 500 measurements per sample, LB-550, Horiba Instruments, Inc., Irvine, CA). The AuNPs were washed twice with 18 MΩ water (Millipore Corp., Billerica, MA) and concentrated by centrifugal filtration. Prior to intravenous injection, they were sterilized by exposure to ultraviolet light for 15 minutes. As there is batch-to-batch variation in AuNPs, all experiments were performed with the same batches of AuNPs. Finally, both solutions of AuNPs remained a dark red wine color during preparation and treatment. Specifically, the color did not change to purple suggesting aggregation of particles.

Vx2, a highly aggressive rabbit squamous cell carcinoma, (Shope and Hurst 1933) was acquired from the Department of Veterinary Medicine and Surgery of The University of Texas M. D. Anderson Cancer Center (MDACC). The tumor was serially passaged by thigh intramuscular injection into New Zealand white rabbits (NZW, Harlan Laboratories, Houston, TX) twice prior to use in the experiments described herein. The MDACC Institutional Animal Care and Use Committee approved all protocols and animal care.

Miscellaneous supplies for blood, urine, and tissue collection were acquired from BD Medical (Franklin Lakes, NJ). Assorted chemicals and laboratory supplies were acquired from Sigma Aldrich Corp. (St. Louis, MO) unless otherwise noted.

Experimental protocol

12 young NZW rabbits (each 3.0 to 3.5 kg) had Vx2 tumors surgically implanted (1.0 – 1.5 mm^3) in an anterior segment of their liver under sterile conditions via a small laparotomy incision according to well developed protocols (Gannon, Cherukuri et al. 2007; Luo, Zhou et al. 2009). Two weeks later, an intrahepatic VX2 tumor 1.0–1.5 cm in diameter was present in all animals. Briefly, Vx2 tumors are very aggressive with nearly 100% uptake. Nearly all tumors are friable and hypervascular with frank central necrosis by 15–20 days after implantation (Luo, Zhou et al. 2009). In our experience, most animals are euthanized for symptomatic pulmonary metastases within 30 to 45 days after implantation. Two weeks after implantation, under general anesthesia the rabbits had a bladder catheter placed along with intraarterial and intravenous catheters in blood vessels in the ears. The rabbits were placed in restrictive boxes (custom built clear plastic animal restraint devices) in order to prevent self-inflicted injury at any of the catheter sites for the remainder of the experiment (25 hours). Next, the rabbits received 1 mg/kg of either 5 nm AuNP (n = 6) or 25 nm AuNP (n = 6) via ear vein injection. At various times after injection, blood was drawn via an ear artery (contralateral ear) and urine was collected via the urinary catheter. Rabbits received a 10 mL/kg intravenous fluid bolus of normal saline 3 and 6 hours after AuNP treatment (and *after* blood/urine was collected for those time points). They were also permitted water and food *ad libitum* during the entire experiment. Twenty-four hours after AuNP injection, the animals were euthanized and a complete necropsy was performed. Representative samples of all major organs were processed using routine histological procedures, embedded in paraffin, and then cut into 5 μm sections. The sections were stained with hematoxylin and eosin (H & E) and examined by light microscopy. In addition, portions of the tumor, spleen, liver, kidneys, and lungs were collected for electron microscopy and gold mass analysis.

Imaging of gold nanoparticles

Gold nanoparticles were imaged with transmission electron microscopy (TEM) post centrifugation. Briefly, tissue samples were fixed with a 3% glutaraldehyde/2% paraformaldehyde solution in 0.1M cacodylate buffer at pH ~ 7.4. Samples were then washed with 0.1% cacodylate buffered tannic acid, treated with 1% buffered osmium tetroxide for 30 minutes, and stained with 1% uranyl acetate. Next the samples were dehydrated with increasing concentrations of ethanol and subsequently embedded in LX-112 medium. After polymerization, the samples were cut with a Leica Ultracut microtome (Leica, Deerfield, IL) and double stained with uranyl acetate/lead citrate in a Leica EM stainer. Samples were imaged with a JEM 1010 TEM (JEOL, USA, Inc., Peabody, MA) at an accelerating voltage of 80 kV. Images were acquired with AMT Imaging System (Advanced Microscopy Techniques Corp., Danvers, MA).

Pharmacokinetics, biodistribution, necropsy and acute toxicity

Whole blood was collected from the contralateral ear artery into evacuated blood collection tubes prior to AuNP injection, at specific time points after injection, and 24 hours after

injection. Samples were then immediately transported to the Department of Veterinary Pathology laboratory where complete cell counts and complete chemistries were performed. Twenty-four hours after AuNP injection, the rabbits were anesthetized with isoflurane and euthanized according to IACUC protocols by Department of Veterinary Medicine and Surgery staff. A complete necropsy was then performed as previously described. An expert in comparative pathology (ANH) performed the necropsy and evaluation for acute toxicity based on gross and histological analysis.

Determination of gold concentration with inductively coupled plasma atomic emission spectrometry (ICP)

Whole blood was collected in heparin coated tubes at specified time points (at time of injection and 10 minutes, 30 minutes, 60 minutes, 2 hours, 3 hours, 6 hours, and 24 hours after injection of AuNPs) via aspiration from an ear artery on the contralateral side of AuNP injection. Urine was collected via a bladder catheter at time points identical to the blood specimen collection.

Tumor and organ specimens (liver, spleen, kidneys, and lung) were sectioned during necropsy, carefully weighed, and prepared for ICP. AuNP levels in blood and urine for pharmacokinetics studies were also measured by ICP. Briefly, 1 mL of whole blood, 5 mL of urine, or ~250 mg of tissue (n = 6 each) was dried at room temperature and weighed. Samples were partially digested with ~ 2 mL certified 30% H_2O_2 and allowed to partially evaporate. Next, 5 mL aqua regia (1 part ACS reagent grade nitric acid combined with 3 parts ACS reagent grade hydrochloric acid by volume, in a fume hood) was slowly added to each sample as the temperature was slowly raised to 130°C in order to completely digest the samples and safely dissolve the gold. After 3 hours, the samples were passively cooled to room temperature and diluted with 18 MΩ water to a final volume of 10 mL. The gold concentration of each sample was determined by ICP according to manufacturers' recommendations (iCAP 6500, Thermo Fisher Scientific, Walthorm, MA).

Statistical analysis

All data represent means while uncertainties are standard errors of the mean, unless otherwise stated. Data were analyzed and plotted with Sigma Plot 11 (Systat Software, Inc., San Jose, CA). Statistical differences between groups were determined with a two tailed, unpaired Student's t-test at a significance level $\alpha = 0.05$. Comparisons between individual rabbit blood cell counts and serum chemistries pre- and post-treatment were performed with a paired Student's t-test.

Results

Size and shape of naked gold nanoparticles

The larger AuNPs (Figure 1A) had a hydrodynamic diameter of 25.7 nm ± 3.9 nm based on DLS (designated "25 nm AuNP" in this manuscript). The smaller particles were below the threshold for accurate measurements of the DLS unit. The smaller AuNPs (Figure 1B) are approximately 5 nm in diameter and predominately spherical in shape with uniform density based on TEM. The larger AuNPs (Figure 1A) have slightly more variation in density and shape than the 5 nm AuNPs. Separate aliquots of well-characterized positive control AuNPs in water did not significantly vary in their expected gold content with a measurement threshold of 0.005 mg/L based on ICP analysis.

Pharmacokinetics of AuNPs

The peak blood concentration of 5 nm AuNPs was 0.53 mg/L ± 0.18 mg/L 10 minutes after injection (Figure 2). The 25 nm AuNPs peaked at 30 minutes at a concentration of 0.11 mg/L ± 0.05 mg/L ($p = 0.048$). Both decreased with time over the next 24 hours.

Urinary excretion of AuNPs

There was a slight biphasic urinary excretion pattern of both the 5 nm AuNPs and the 25 nm AuNPs (Figure 3). A small peak occurred at 30 minutes with concentrations of 0.60 mg/L ± 0.01 mg/L for 5 nm AuNP and 0.35 mg/L ± 0.10 mg/L for 25 nm AuNP ($p = 0.032$), respectively. A second, larger peak occurred at 6 hours (360 minutes) after injection in both groups. The gold concentration in urine at 6 hours was 1.03 mg/L ± 0.91 mg/L for 5 nm AuNP and 1.93 mg/L ± 0.10 mg/L ($p = 0.35$) for 25 nm AuNP, respectively.

Biodistribution of AuNPs

Splenic tissue contained significantly more 5 nm gold than 25 nm gold on a milligram gold per gram tissue basis (Figure 4, $p = 0.003$). However, although liver and tumor tissues contained relatively more 25 nm AuNP than 5 nm AuNP, this was not statistically significant ($p = 0.18$ for liver and $p = 0.24$ for tumor). Splenic and liver tissue contained significantly more 5 or 25 nm AuNPs than lung and kidney tissue (Figure 4, $p < 0.001$). Tumor tissue contained more 25 nm AuNPs than either lung or kidney (Figure 4, $p \sim 0.085$ for each). Tumor tissue did not contain significantly more 5 nm AuNPs than lung (Figure 4, $p = 0.16$), but there was a trend towards increased concentration of 5 nm AuNP in tumor compared to kidney tissue ($p=0.0508$). TEM qualitatively demonstrates AuNP distribution in representative images of liver and Vx2 tumor 24 hours after treatment with 25 nm AuNP (Figure 5).

Acute toxicity of AuNP

There were no significant gross or histological lesions associated with toxicity of AuNPs found in any examined organs. Furthermore, extra sections of the liver and spleen were analyzed because of the unique tissue architecture that these organ have, and no abnormalities were found. In addition, there were no major clinical changes in the behavior of the rabbits, eating habits, or unusual postures (classical signs of distress in rabbits). Blood, taken soon after euthanasia, revealed a minimally elevated white blood cell (WBC) count after treatment with 25 nm AuNP (Table 1). The differential WBC demonstrated an increase in segmented neutrophils and a decreased lymphocyte count (Table 1). Liver function tests (ALT, AST, alkaline phosphatase, and bilirubin) and renal function (creatinine) remained within the normal range (Table 1). Serum creatine kinase (CK) levels were elevated 2x compared to pretreatment values only in rabbits treated with 25 nm AuNPs.

Vx2 lesions were confined to the liver implantation site of all rabbits. The lesions consisted of locally extensive areas of tumor formation at the site of inoculation (Fig. 6A). Microscopic examination of the tumor tissue revealed sheets of Vx2 neoplastic cells that had large round to oval nuclei with indistinct cell borders (Fig. 6B). Neoplastic cells showed cellular atypia and many mitotic figures (up to 20 per high magnification, x40). Also, there were extensive areas of multifocal necrosis within the neoplastic tissue (Fig. 6C) indicating a rapidly growing tumor out-growing its available blood supply. Additionally, small foci of metastatic tumor cell were present in lungs of 8 out of 12 rabbits. One animal in the 25 nm AuNPs treated group had Vx2 neoplastic cells on the serosal surface of colon.

Non-clinically significant lymphoid lesions (lymphoid aggregates or lymphoid hyperplasia) were found in the lung, liver, and pancreas after treatment with 5 nm AuNP. Similar non-

significant lesions were found in the lung, pancreas, and small bowel after treatment with 25 nm AuNPs.

Discussion

AuNPs appear to be safe with no histologic evidence of lesions or inflammatory changes related to acute toxicity 24 hours after treatment in rabbits. Specifically, we did not find any changes in the architecture of the liver or spleen. These two organs have a high volume of tissue macrophages and often collect foreign particles in the reticuloendothelial system (RES). However, the rabbits here did not demonstrate any morphological or histological evidence of toxicity. Interestingly, the mild (and sometime major) toxicity of other, non-gold nanoparticles was not demonstrated here (Trouiller, Reliene et al. 2009; Johnston, Hutchison et al. 2010). While gold salts have mild toxicity and non-gold nanoparticles may have some toxicity, solid metallic gold nanoparticle may be of the proper size and surface chemistry to avoid pathology-inducing interactions.

While gold salts are typically associated with renal toxicity, (Antonovych 1981) there was very little AuNPs found in the kidneys 24 hours after intravenous injection despite significant levels in the urine. This is reassuring since the toxicity of gold salts is believed to be caused by the presence of ionic gold. We hypothesize that the stable serum creatinine level and low concentration found in the renal parenchyma is indicative that metallic AuNPs will have minimal renal toxicity. The small size of the AuNPs compared to colloidal gold preparations should allow easy passage and clearance through glomeruli and renal tubules.

The increase in creatine kinase (CK) was an unexpected finding. CK elevation is typically associated with muscle injury. On gross and histological evaluation, there was no evidence of muscle or other tissue injury. This finding may be associated with animals undergoing anesthesia being restrained for 25 hours. We suggest only that when AuNPs reach clinical trials this toxicity should be fully evaluated.

Interestingly, the increase in white blood cell count was predominately due to a 14.6% ± 2.9% increase in segmented neutrophils (polymorphonuclear leukocytes). The rabbits did not demonstrate evidence clinically (i.e. change in eating habits) or pathologically of infection, so it appears that this denotes a non-specific inflammatory reaction to AuNP injection. Although a possibility, we think that it is unlikely that this represents an infection because the animals would demonstrate a clinically evident response to a blood infection (i.e., sepsis), which was not seen. This may also be a generalized stress response to multiple procedures and the experimental protocol. Finally, it should be noted that limited UV light exposure may have been inadequate to fully sterilize the solution, but is necessary as extensive UV light exposure may induce AuNP aggregation.

AuNPs are distributed to the liver and spleen significantly more so than lung and kidney tissue. As the liver and spleen are much larger than the kidneys, lungs, or tumor, the vast majority of gold is distributed to those two organs both by concentration and total mass. Vx2, a rabbit carcinoma used to model hepatocellular carcinoma here, contained more gold than lung or kidney, suggesting that the “leaky tumor vessels” may play a minor role in non-specific uptake (Hashizume, Baluk et al. 2000). Increasing circulating times (i.e., with PEGylation) may increase non-specific tumor delivery, and may reduce sequestration by the RES in the liver and spleen during that time. However, liver tissue contained significantly more AuNPs suggesting that relying on porous neovasculature within solid tumors alone is not selective enough to be a reasonable method for nanoparticle delivery to treat malignant tumors. We did not measure AuNP in brain tissue but it is known that a very small fraction of 12.5 nm AuNPs cross the blood brain barrier (Lasagna-Reeves, Gonzalez-Romero, et al.

2010). TEM demonstrated that the AuNPs are primarily located in the cytoplasm while ICP described the total concentration. However, other techniques such as micro- x-ray fluorescence often can yield useful simultaneous data. However, TEM resolution is higher.

We hypothesize that the larger AuNPs (25 nm) were found at higher concentrations, despite a lower molar concentration, because of multiple factors. First, the initial urinary excretion of 5 nm AuNPs was higher than the larger AuNPs. Obviously, the more rapidly excreted AuNPs have lower mass concentration in the blood. Likewise, splenic tissue took up more 5 nm AuNPs than 25 nm AuNPs. For similar reasons, we hypothesize that once an AuNP is sequestered in the spleen, it remains there.

Based on whole blood levels of naked AuNPs, these particles will stay in the blood circulation for up to 6 hours, with much higher concentrations for the first ~3 hours. Although it is difficult to compare the exposure time needed for nonspecific cellular internalization of AuNPs, previous *in vitro* results suggested that an internalization plateau is reached ~ 4 hours after treatment (Chithrani, Ghazani et al. 2006). This is congruent with our *in vivo* data that high concentration exposure (as measured by gold concentration in the blood) is similar (~ 3 to 6 hours) to peak *in vitro* exposure duration. Obviously, antibody, peptide, and other functionalizations utilized in targeting AuNPs cancer cells specifically may change these timelines. Furthermore, it is possible that pegylation (to prolong circulating half-life) will not be required with AuNP constructs if non immunogenic cancer targeting antibodies and peptides are conjugated to the surface of AuNPs. Side effect profiles of AuNPs in humans will need to be established. However, rapid renal excretion of the AuNPs is likely to be beneficial to avoid toxicity. Furthermore, if internalization of AuNPs into cancer cells peaks by the time excretion is significant, the net effect is a potentially robust delivery system.

While we utilized equal mass concentrations of AuNPs, the different sized AuNPs have different surface areas as well as different molar concentrations. This may compound the results in two ways, at least. First, the smaller mass coupled with higher surface area per mass in the 5nm AuNP permit higher rates of interaction with the surronding mileiu if correlated to mass of gold. Since the mechanisms of nanoparticle distribution and interactions, in general, are still being fully elucidated, it is difficult to state exactly the consequences. We chose treatments based on mass concentration because standard pharmacologic interventions are often dosed as mg per kg in the clinic.

This study does not evaluate the toxicity of long-term or repeated AuNP treatments and does not completely describe the role of the enteric-biliary-fecal circulation. Interestingly, there was no biochemical or histopathological evidence of hepatobiliary injury or congestion. We do not expect that long-term treatments will have increased hepatic toxicity due to liver deposition, especially since Kupffer cells will likely ingest most of the metallic nanoparticles (Sadauskas, Wallin et al. 2007; Sadauskas, Danscher et al. 2009). Additionally, since AuNPs pass through the kidneys, it may be possible to wash out the AuNP with concomitant administration of intravenous or oral fluids (as was performed here) without collecting excess AuNPs in renal parenchyma, hence avoiding long-term renal toxicity. Finally, the effects in ionizing and magnetic radiation (i.e., CT and MRI) in the presence of metal nanoparticles will need to be investigated clinically as well.

We have demonstrated that 25 nm gold nanoparticles distribute more evenly between the liver, spleen, and tumor tissue in this *in vivo* model of liver cancer. 5 nm AuNPs, however, were found at much higher concentrations in the liver. Regardless, the AuNPs seem to be safely tolerated with no significant evidence of acute toxicity.

Acknowledgments

Funding sources: This work was partially funded from the NIH (U54CA143837 and Core Grant CA16672) and an unrestricted research grant from the Kanzius Foundation (SAC, Erie, PA). In addition, ESG is an NIH T32 research fellow (T32 CA09599).

The authors would like to acknowledge the staff and animal care technologists of the Department of Veterinary Medicine and Surgery, specifically Maurice J Dufilho, IV and Darla Y. Stange for assistance with necropsy and Vx2 cell culture. Kenneth Dunner, Jr., of The High Resolution Electron Microscopy Facility at The University of Texas M.D. Anderson Cancer Center provided valuable assistance with TEM imagining. The authors would also like to thank Kristine Ash and Yolanda Brittain for administrative support.

References

Antonovych TT. Gold nephropathy. Ann Clin Lab Sci. 1981; 11(5):386–91. [PubMed: 7036839]

Bar-Ilan O, Albrecht RM, et al. Toxicity assessments of multisized gold and silver nanoparticles in zebrafish embryos. Small. 2009; 5(16):1897–910. [PubMed: 19437466]

Cherukuri P, Glazer ES, et al. Targeted hyperthermia using metal nanoparticles. Adv Drug Deliv Rev. 2009

Chien AJ, Illi JA, et al. A phase I study of a 2-day lapatinib chemosensitization pulse preceding nanoparticle albumin-bound Paclitaxel for advanced solid malignancies. Clin Cancer Res. 2009; 15(17):5569–75. [PubMed: 19706807]

Chithrani BD, Ghazani AA, et al. Determining the size and shape dependence of gold nanoparticle uptake into mammalian cells. Nano Lett. 2006; 6(4):662–668. [PubMed: 16608261]

Curley SA, Cherukuri P, et al. Noninvasive radiofrequency field-induced hyperthermic cytotoxicity in human cancer cells using cetuximab-targeted gold nanoparticles. J Exp Ther Oncol. 2008; 7(4):313–26. [PubMed: 19227011]

De Jong WH, Hagens WI, et al. Particle size-dependent organ distribution of gold nanoparticles after intravenous administration. Biomaterials. 2008; 29(12):1912–9. [PubMed: 18242692]

Decuzzi P, Ferrari M. The receptor-mediated endocytosis of nonspherical particles. Biophys J. 2008; 94(10):3790–7. [PubMed: 18234813]

Dhar S, Daniel WL, et al. Polyvalent oligonucleotide gold nanoparticle conjugates as delivery vehicles for platinum(IV) warheads. J Am Chem Soc. 2009; 131(41):14652–3. [PubMed: 19778015]

Finkelstein AE, Walz DT, et al. Auranofin. New oral gold compound for treatment of rheumatoid arthritis. Ann Rheum Dis. 1976; 35(3):251–7. [PubMed: 791161]

Gannon CJ, Cherukuri P, et al. Carbon nanotube-enhanced thermal destruction of cancer cells in a noninvasive radiofrequency field. Cancer. 2007; 110(12):2654–65. [PubMed: 17960610]

Glazer ES, Curley SA. Radiofrequency field-induced thermal cytotoxicity in cancer cells treated with fluorescent nanoparticles. Cancer. 2010; 116(13):3285–93. [PubMed: 20564640]

Hashizume H, Baluk P, et al. Openings between defective endothelial cells explain tumor vessel leakiness. Am J Pathol. 2000; 156(4):1363–80. [PubMed: 10751361]

Ibrahim NK, Desai N, et al. Phase I and pharmacokinetic study of ABI-007, a Cremophor-free, protein-stabilized, nanoparticle formulation of paclitaxel. Clin Cancer Res. 2002; 8(5):1038–44. [PubMed: 12006516]

Johnston HJ, Hutchison G, et al. A review of the in vivo and in vitro toxicity of silver and gold particulates: particle attributes and biological mechanisms responsible for the observed toxicity. Crit Rev Toxicol. 2010; 40(4):328–46. [PubMed: 20128631]

Lasagna-Reeves C, Gonzalez-Romero D, et al. Bioaccumulation and toxicity of gold nanoparticles after repeated administration in mice. Biochem Biophys Res Commun. 2010; 393(4):649–55. [PubMed: 20153731]

Luo W, Zhou X, et al. Role of sonography for implantation and sequential evaluation of a VX2 rabbit liver tumor model. J Ultrasound Med. 2009; 29(1):51–60. [PubMed: 20040775]

Milacic V, Fregona D, et al. Gold complexes as prospective metal-based anticancer drugs. Histol Histopathol. 2008; 23(1):101–8. [PubMed: 17952862]

Sadauskas E, Danscher G, et al. Protracted elimination of gold nanoparticles from mouse liver. Nanomedicine. 2009; 5(2):162–9. [PubMed: 19217434]

Sadauskas E, Wallin H, et al. Kupffer cells are central in the removal of nanoparticles from the organism. Part Fibre Toxicol. 2007; 4:10. [PubMed: 17949501]

Shope RE, Hurst EW. Infectious Papillomatosis of Rabbits: With a Note on the Histopathology. J Exp Med. 1933; 58(5):607–624. [PubMed: 19870219]

Sonavane G, Tomoda K, et al. Biodistribution of colloidal gold nanoparticles after intravenous administration: effect of particle size. Colloids Surf B Biointerfaces. 2008; 66(2):274–80. [PubMed: 18722754]

Sukumar M, Doyle BL, et al. Opalescent appearance of an IgG1 antibody at high concentrations and its relationship to noncovalent association. Pharm Res. 2004; 21(7):1087–93. [PubMed: 15290846]

Trouiller B, Reliene R, et al. Titanium dioxide nanoparticles induce DNA damage and genetic instability in vivo in mice. Cancer Res. 2009; 69(22):8784–9. [PubMed: 19887611]

Wust P, Gneveckow U, et al. Magnetic nanoparticles for interstitial thermotherapy--feasibility, tolerance and achieved temperatures. Int J Hyperthermia. 2006; 22(8):673–85. [PubMed: 17390997]

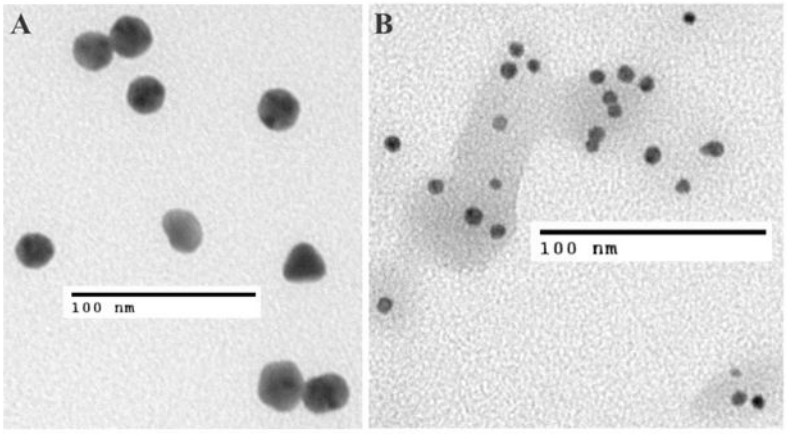

Figure 1.
Transmission electron microscopic images of stock 25 nm gold nanoparticles (A) and 5 nm gold nanoparticles (B) in water demonstrate that they are circular, solid, and fairly uniform nanoparticles with a few obvious exceptions.

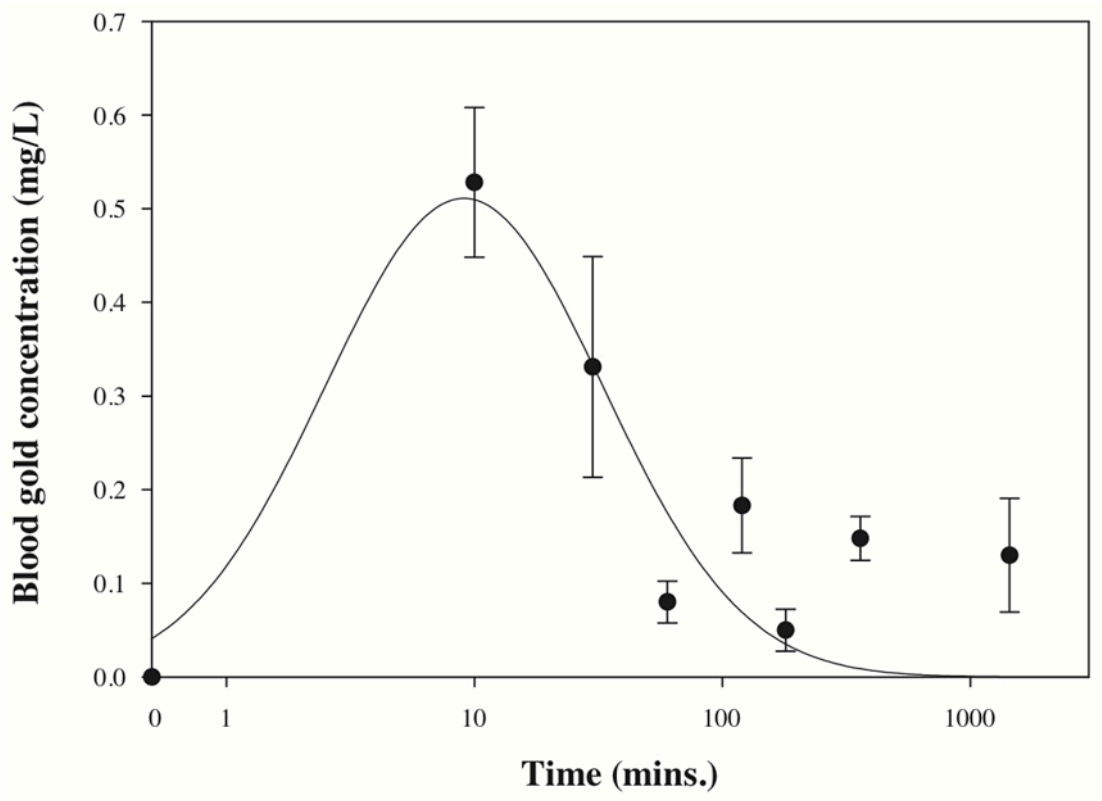

Figure 2.

ICP demonstrates that after intravenous injection of 5 nm gold nanoparticles (n = 6 rabbits) blood levels peak approximately 10 minutes after injection as measured at the contralateral ear artery. Less than 20% remained in circulation after 24 hours. Error bars are standard error of the mean for n = 6 rabbits. The logarithmic x-axis was modified to include a time = 0 point at the origin of the graph.

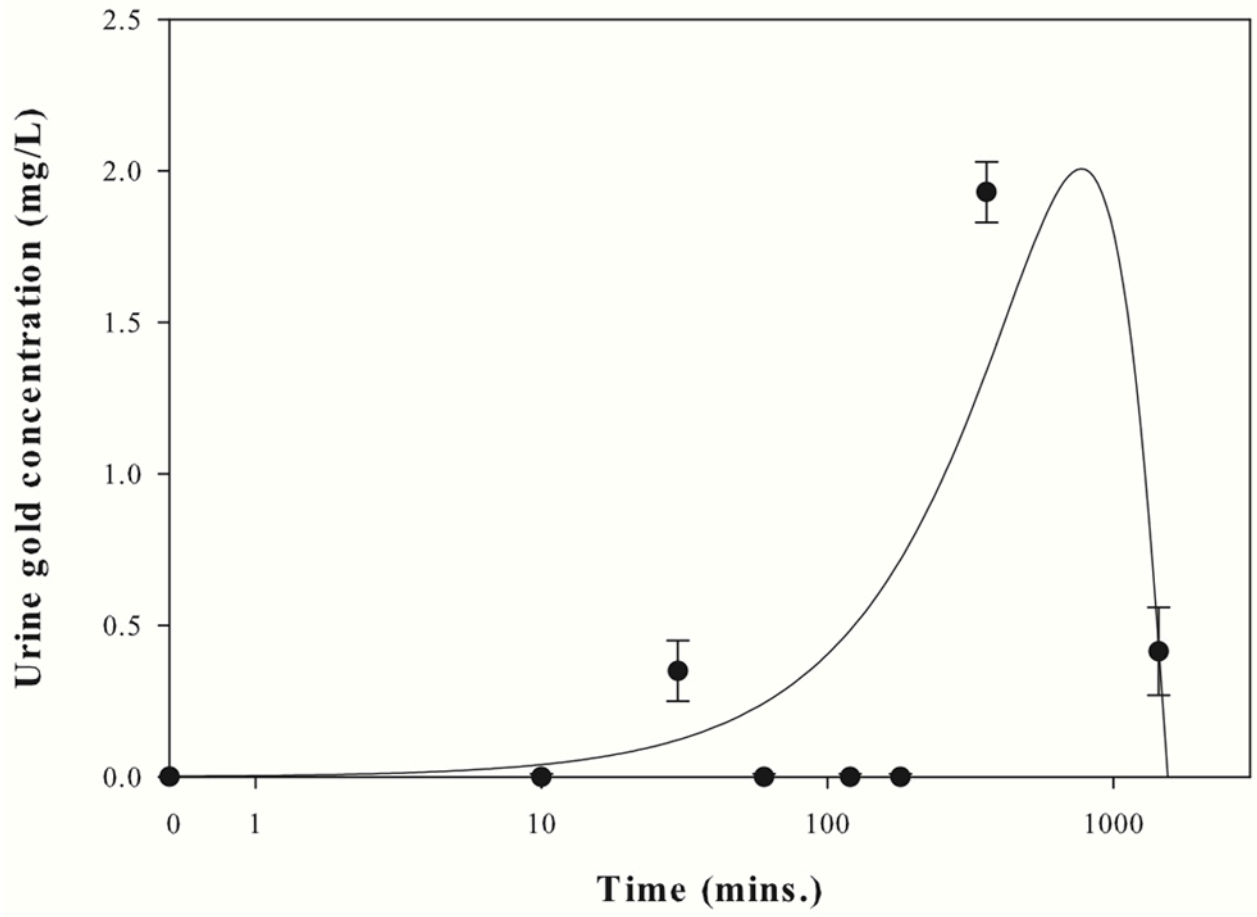

Figure 3.

ICP demonstrates that the urinary excretion of ~25 nm gold nanoparticles is slightly biphasic with a small peak approximately 30 minutes after injection and much higher peak 180 minutes (6 hours) after injection. Error bars are standard error of the mean for n = 6 rabbits. The logarithmic x-axis was modified to include a time = 0 point at the origin of the graph.

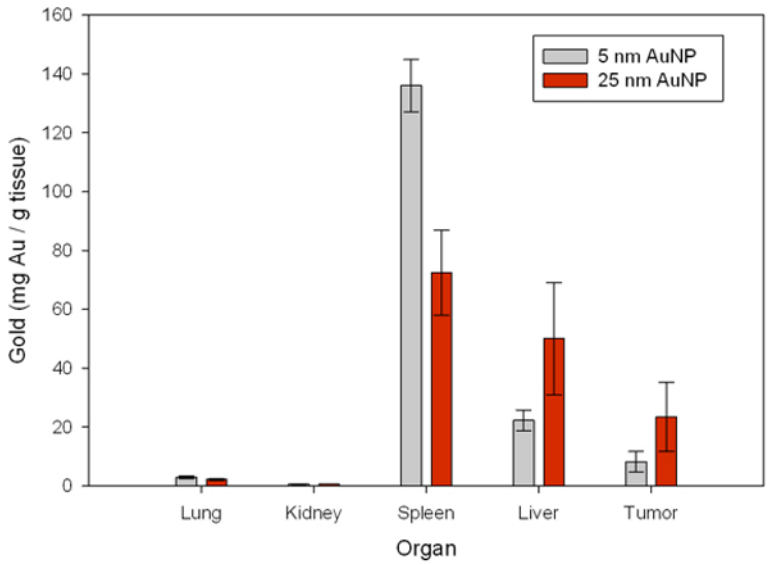

Figure 4.

The biodistribution of gold nanoparticles as measured by ICP demonstrate higher uptake of 5 nm gold nanoparticles in the spleen while both the liver and tumor contained higher levels of 25 nm gold nanoparticles by weight. N = 6 for each group.

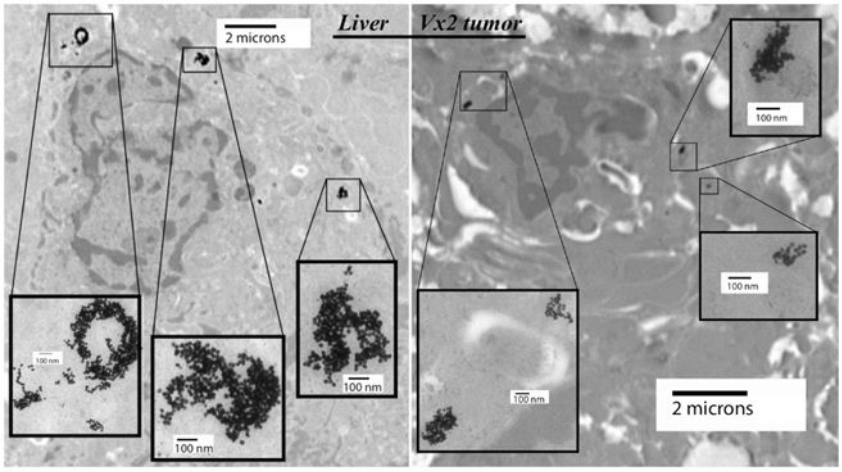

Figure 5.
TEM images of the liver (left) and Vx2 tumor (right) 24 hours after injection of 25 nm gold nanoparticles demonstrates qualitatively the distribution seen quantitatively in Figure 4.

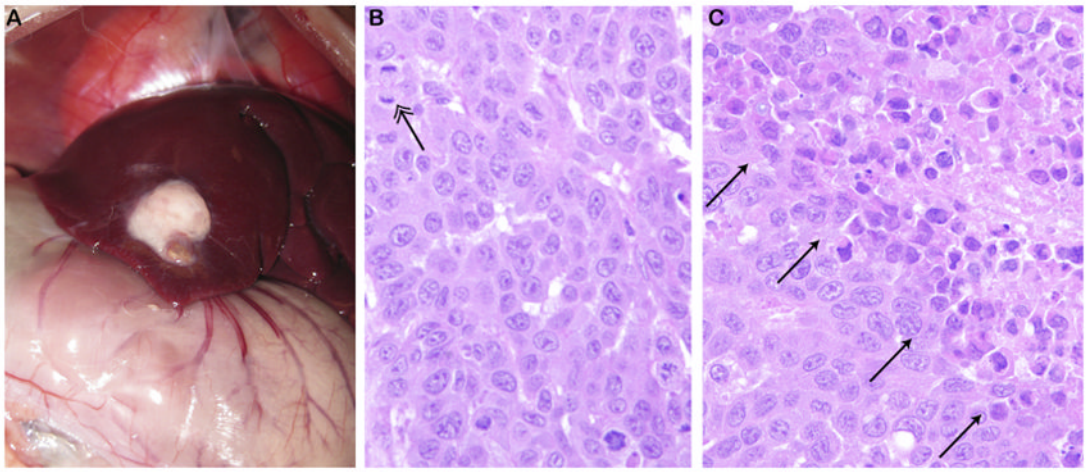

Figure 6.

Gross image of Vx2 tumor implanted in liver (A), microscopic image of the tumor (magnified x40, H&E stained, B), and of a foci of necrosis within the neoplastic tissue (magnified x40, H&E stained, C). The double arrow head (B) demonstrates one of the mitotic figure while the arrows (C) demonstrate the demarcation between necrotic zones (upper right) and viable regions (lower left).

Table 1

In general, most laboratory blood values before and after treatment with gold nanoparticles were not statistically different. However, there was a significant increase in the white blood cell (WBC) count and creatine kinase (CK) after treatment with 25 nm AuNP. In contrast, there was a statistically significant decrease in the platelet count and alkaline phosphatase in the blood after treatment with 5 nm AuNP

	5 nm AuNP			*25 nm AuNP*		
Laboratory Study	**Pre-treatment (mean ± SEM)**	**Post-treatment (mean ± SEM)**	**p value**	**Pre-treatment (mean ± SEM)**	**Post-treatment (mean ± SEM)**	**p value**
WBC ($\times 10^3/\mu L$)	8.8 ± 0.8	10.2 ± 1.4	0.420	9.1 ± 0.9	12.9 ± 0.7	**0.001**
Segmented Neutrophils	31.2% ± 3.8%	42.9% ± 10.2%	0.212	31.2% ± 4.6%	48.6% ± 6.0%	0.057
Lymphocytes	57.2% ± 4.2%	47.1% ± 10.1%	0.665	58.3% ± 5.2%	40.3%± 6.2%	0.077
Platelet ($\times 10^3/\mu L$)	474 ± 28	188 ± 87	**0.005**	390 ± 41	429 ± 57	0.292
Lipase (U/L)	446 ± 41	458 ± 33	0.860	335 ± 35	288 ± 26	0.384
Creatinine (mg/dL)	0.92 ± 0.08	0.83 ± 0.05	0.406	1.31 ± .09	1.16 ± .08	0.133
CK (U/L)	650 ± 219	1234 ± 267	0.132	395 ± 39	732 ± 118	**0.016**
ALT (U/L)	40.0 ± 4.6	41.0 ± 6.2	0.894	34.7 ± 3.3	35.0 ± 1.9	0.869
Alkaline Phosphatase (U/L)	78.7 ± 3.2	55.0 ± 3.8	**0.001**	50.0 ± 8.1	47.3 ± 8.8	0.674
Lactate Dehydrogenase (U/L)	35.3 ± 1.9	176.7 ± 93.6	0.193	68.2 ± 10.9	110.2 ± 45.6	0.327
Billirubin (mg/dL)	0.1 ± 0.0	0.1 ± 0.0	1.000	0.1 ± 0.0	0.12 ±.02	0.363

ALT: alanine aminotransferase, SEM: standard error of the mean.

In addition to this table, there were no significant differences in the following blood values for either treatment group: red blood cell count/volume/size, serum electrolytes (Na, K, Cl, Ca, P, Mg), glucose, blood urea nitrogen, aspartate transaminase, lactate dehydrogenase, or gamma glutamyl transferase,